

# Convection-driven geodynamo models

BY C. A. JONES

*School of Mathematical Sciences, University of Exeter, Exeter EX4 4QE, UK*

There has been significant progress in the development of numerical geodynamo models over the last five years. Advances in computer technology have made it possible to perform three-dimensional simulations, with thermal or compositional convection as the driving mechanism. These numerical simulations give reasonable results for the morphology and strength of the field at the core–mantle boundary, and the models are also capable of giving reversals and excursions which can be compared with palaeomagnetic observations; they also predict differential rotation between the inner core and the mantle.

However, there are still a number of fundamental problems associated with the simulations, which are proving hard to overcome. Despite the advances in computing power, the models are still expensive and take a long time to run. This problem may diminish as faster machines become available, and new numerical methods exploit parallelization effectively, but currently there are no practical schemes available which work at low Ekman number.

Even with turbulent values of the diffusivities (and the question of whether isotropic diffusivities are appropriate is still unresolved), the appropriate dynamical regime has not yet been reached. In consequence, modelling assumptions about the nature of the flow near the boundaries have to be made, and different choices can have profound effects on the dynamics. The nature of large-scale magnetoconvection at small  $E$  is still not well understood, and until we have more understanding of this issue, it will be difficult to have a great deal of confidence in the predictions of the numerical models.

**Keywords:** dynamo; Earth's core; rotating convection

---

## 1. Introduction

In the past ten years there has been considerable activity in geodynamo modelling, the main effort being directed towards convection-driven geodynamo models. Very significant progress has been achieved; models constructed from solutions of the Navier–Stokes and Maxwell equations can now be sensibly compared with geophysical observations of the actual geomagnetic field. Results obtained from palaeomagnetic data, such as the nature of the reversals of the main field, can also be modelled directly from the fundamental equations (Sarson & Jones 1999; Glatzmaier *et al.* 1999). Despite this undoubted progress, there are still a number of fundamental problems which remain unresolved. The parameter regime in which the current generation of numerical models can be run is very far from the regime of geophysical parameter values; so far, indeed, that the strong similarity between the model outputs and the geodynamo is quite surprising.

The rotating spherical shell model is a natural problem to study as a geodynamo model, and a considerable number of papers have been based on it; we refer to it here as the ‘zero-order model’ because it is a clear-cut mathematical problem, although it should be emphasized that physical effects not included in the zero-order model may be very significant for the real geodynamo. In the zero-order model there is just one source of buoyancy, whereas in the geodynamo there are two, thermal and compositional buoyancy. We also assume homogeneous spherically symmetric boundary conditions, whereas in the geodynamo mantle convection is spatially inhomogeneous. Heat flux absorbed by the mantle will be a function of the spherical polar coordinates  $\theta$  and  $\phi$ , which is determined mainly by the dynamics of mantle convection (Zhang & Gubbins 1993; Olson & Glatzmaier 1995), and this can affect dynamo action (Sarson *et al.* 1997*a*; Glatzmaier *et al.* 1999). There is also a considerable density variation between the inner-core boundary (ICB) and the core–mantle boundary (CMB), but this is ignored in the Boussinesq zero-order model.

Even within the zero-order model, there are a number of choices to be made; the buoyancy source can be distributed uniformly throughout the inner core (the uniform heating model) or put entirely in the inner core through a flux at the ICB. The boundary conditions can be taken as no-slip or stress-free; various options can be taken to model the inner core. Sometimes it is neglected altogether, and convection in a whole sphere is considered; sometimes the inner core is given its current size (about 0.35 times the radius of the outer core) but it is assumed to be electrically insulating; and sometimes it is allowed to be electrically conducting, usually with a similar conductivity to that of the outer core. The resulting dynamo behaviour is strongly affected by which of these choices is made.

A strong motivation for the activity in geodynamo modelling is the possibility of using the models to compare with geophysical measurements. Secular variation studies and palaeomagnetic observations are two important examples, but dynamo models might also help us to understand the physical conditions at the CMB. Another exciting application is to apply our understanding of the geodynamo to the magnetic fields of other planets; the recently discovered internal fields on the Jovian moons Ganymede and Io (Schubert *et al.* 1996; Sarson *et al.* 1997*b*) are prime candidates to test dynamo models.

In this paper, we concentrate on interpreting and understanding results from the zero-order models, and on trying to relate these results to the actual geodynamo. The models need to be fully validated before we can reliably use them as a tool for further geophysical studies.

Previous reviews on the dynamics and magnetohydrodynamics of the Earth’s core include Fearn (1998), Glatzmaier & Roberts (1997), Hollerbach (1996) and Braginsky (1994). Dynamo theory was reviewed by Roberts & Soward (1992) and Roberts (1994) and more background information can be found in Roberts & Gubbins (1987).

## 2. The zero-order model and governing equations

We consider an electrically conducting Boussinesq fluid layer confined between two concentric spherical surfaces, at  $r = r_1$  (corresponding to the ICB) and at  $r = r_o$  (corresponding to the CMB) in a frame rotating at angular velocity  $\Omega_0$ , which we identify with the mantle frame. The inner core is taken as a solid electrically conducting sphere concentric with the outer core, which is free to rotate about the  $z$ -axis at

angular velocity  $\Omega_i$  relative to the mantle frame. We denote the density deficit due to compositional or thermal variations as  $C$ , the codensity. The codensity source, which drives the convection, is denoted by  $S$ . This source leads to a codensity difference  $\Delta C$  across the fluid outer core. The distance between the surfaces  $d = r_o - r_i = 2260$  km is taken as the length-scale, the time-scale is the magnetic diffusion time  $d^2/\eta \approx 80$  kyr, the magnetic field unit is  $(2\Omega_o\rho\mu\eta)^{1/2} \approx 20$  Gauss (where  $\rho$  is the fluid density,  $\mu$  is the permeability and  $\eta$  is the magnetic diffusivity) and the codensity unit is  $\Delta C$ . The governing MHD equations for the velocity  $\mathbf{u}$ , the magnetic field  $\mathbf{B}$  and the codensity  $C$  are

$$\frac{E}{qPr} \frac{D\mathbf{u}}{Dt} + \hat{\mathbf{z}} \times \mathbf{u} = -\nabla p + \mathbf{j} \times \mathbf{B} + E\nabla^2\mathbf{u} + qRaCr, \quad (2.1)$$

$$\frac{\partial \mathbf{B}}{\partial t} = \nabla^2 \mathbf{B} + \nabla \times (\mathbf{u} \times \mathbf{B}), \quad (2.2)$$

$$\frac{\partial C}{\partial t} = q\nabla^2 C - \mathbf{u} \cdot \nabla C + S, \quad (2.3)$$

$$\nabla \cdot \mathbf{B} = 0, \quad (2.4)$$

$$\nabla \cdot \mathbf{u} = 0. \quad (2.5)$$

Here  $\mathbf{j} = \nabla \times \mathbf{B}$  is the current, and the dimensionless parameters are the Ekman number  $E = \nu/2\Omega_o d^2$ , the Prandtl number  $Pr = \nu/\kappa$ , the Roberts number  $q = \kappa/\eta$  and the Modified Rayleigh number  $R = g\alpha\Delta T d/2\Omega_o\kappa$ . In these definitions,  $\nu$  is the kinematic viscosity and  $\kappa$  is the codensity diffusivity. Other combinations of the parameters are sometimes used, notably the magnetic Prandtl number  $Pr_m = \nu/\eta = qPr$  and non-rotating Rayleigh number  $Ra = g\alpha\Delta T d^3/\kappa\nu = R/E$ .

In addition we have two further dimensionless parameters, the radius ratio  $r_i/r_o$ , which is usually taken to be around 1/3 to model the geodynamo, and the magnetic diffusivity ratio of the outer to the inner core,  $\eta_o/\eta_i$ . The most popular choice is  $\eta_o/\eta_i = 1$ , which we call a conducting inner core.

In the conducting-inner-core case, we need to solve for the magnetic field  $\mathbf{B}_i$  and the angular velocity  $\Omega_i$ . The inner-core magnetic field is governed by

$$\frac{\partial \mathbf{B}}{\partial t} + \Omega_i \frac{\partial \mathbf{B}}{\partial \phi} = \frac{\eta_i}{\eta_o} \nabla^2 \mathbf{B}. \quad (2.6)$$

The mechanical boundary conditions are that there should be no flow through the ICB and CMB surfaces, and that there should be no-slip at these surfaces, so  $\mathbf{u} = \mathbf{0}$  at the CMB and  $\mathbf{u} = \Omega_i \hat{\mathbf{z}} \times \mathbf{r}$  at the ICB. Alternatively, stress-free conditions can be applied at the ICB, CMB or both (Kuang & Bloxham 1997).

Thermal boundary conditions must also be applied. Popular choices are  $C$  constant on  $r = r_i$  and  $r = r_o$ , or fixed flux boundary conditions, or some combination of the two. Another common choice is to assume a uniform source in the outer core, together with fixed codensity boundaries. The non-magnetic problem with a fixed codensity (usually heat) source has been extensively studied.

The magnetic boundary conditions are that the normal component of  $\mathbf{B}$  and the tangential components of the electric field  $\mathbf{E}$  are continuous. The latter conditions can easily be converted into conditions on the current using the MHD form of Ohm's law. Note that if stress-free rather than no-slip conditions are used at a conducting boundary, then the velocity on the boundary will enter the magnetic boundary conditions through Ohm's law.

The angular velocity  $\Omega_i$  is determined by the torque balance at the ICB. In general, the rate of change of the angular momentum of the inner core is determined by adding the magnetic torque, the viscous torque and any external torque, such as a gravitational torque. Buffett (1997) has argued that asymmetries in the mantle give rise to asymmetries in the shape of the inner core, and that the resulting gravitational torque can be even larger than the magnetic torque. In the stress-free case, the viscous torque is zero, so the rate of change of angular momentum of the inner core is then determined solely by magnetic and external torque. Estimates of the moment of inertia of the inner core and the likely order of magnitude of the magnetic torque suggest that the inner core can spin up due to magnetic torque in a few days; on the dynamo time-scale the inner core will therefore be in torque equilibrium. If the viscous torque is small, this means that the total magnetic and external torque must be zero; any torque supplied to one region of the ICB must be balanced by an opposite torque somewhere else, so that the torque surface integral adds up to zero; this has been called the ‘inner-core Taylor constraint’.

With this scaling, the dimensionless strength of the magnetic field gives a local measure of the Elsasser number,  $\Lambda = B^2/2\mu\rho\Omega_0\eta$ . Although the Elsasser number is only a derived quantity and not an input parameter, it is useful for comparison with magnetoconvection models where  $\Lambda$  is an input parameter. Similarly, the dimensionless strength of the velocity field gives a local measure of the magnetic Reynolds number  $R_m = ud/\eta$ . Again, this is a derived quantity, but it is very useful to compare its value with the results of kinematic dynamo models, where  $R_m$  is an input parameter.

### 3. Numerical methods

The most popular technique for solving the dynamo equations numerically has been the pseudo-spectral method, recently described by Cox & Matthews (1997) and Hollerbach (2000), and applied to the geodynamo by Glatzmaier & Roberts (1995) and Kuang & Bloxham (1999). The vector fields  $\mathbf{u}$  and  $\mathbf{B}$  are expanded into toroidal and poloidal parts, and these scalar fields, together with the  $C$  field, are expanded in spherical harmonics. In the radial direction either a finite difference scheme or expansion in Chebyshev polynomials is used. These expansions are inserted into (2.1)–(2.5) and time-dependent equations for the coefficients are obtained. The linear diffusion operators are handled using an implicit scheme, such as the Crank–Nicholson method, while the nonlinear terms are handled explicitly by converting from spectral space to physical space so that the required multiplications can be handled easily. This procedure leads to accurate solutions provided moderate parameter values are used; it does, however, require large computing resources. In addition to the obvious problem associated with computing fully three-dimensional numerical solutions, there are two additional problems which make the execution times even longer: first, there is no efficient fast Legendre transform, as there is for Fourier transforms, and second, at small  $E$  the time-step has to be very small (see Walker *et al.* (1998) for details).

Motivated by these difficulties, a number of ways of reducing the CPU time required have been tried. One method has been to truncate the equations severely in the azimuthal direction, sometimes leaving only the axisymmetric and one non-axisymmetric  $e^{im\phi}$  mode; this is known as the  $2\frac{1}{2}$ -dimensional method. This tech-

nique reduces the CPU time required by a large factor. The disadvantage of this method is that the non-axisymmetric wavenumber  $m$  has to be chosen *a priori*, rather than emerging from the calculation. Nevertheless, the axisymmetric fields generated by the  $2\frac{1}{2}$ -dimensional method are remarkably close to those computed by fully three-dimensional calculations provided the azimuthal wavenumber is chosen sensibly: in the limited parameter regimes that can be explored numerically, choosing  $m$  as the first mode to become linearly unstable as  $R$  is increased is normally an adequate choice. The  $2\frac{1}{2}$ -dimensional approach is therefore a useful tool in exploring dynamo behaviour, but one can only have full confidence in the results if they are calibrated by at least some fully three-dimensional simulations. The simulations used for figures 2 and 3 below are a compromise between the  $2\frac{1}{2}$ -dimensional model and fully three-dimensional simulations; the  $r$  and  $\theta$  directions are fully resolved, but a small number of non-axisymmetric modes (typically four) are present, together with the axisymmetric modes.

Another popular technique has been the use of hyperdiffusion to reach lower Ekman number solutions. Here the diffusive operator  $\nabla^2$  is replaced by some formula such as  $(1 + \lambda n^3)\nabla^2$ , where  $n$  is the order of the spherical harmonic in the expansion of the fields and  $\lambda$  is a constant. This method is very simple to implement if the pseudo-spectral method is used, and it stabilizes the numerical scheme for values of  $\lambda \sim 0.05$ , allowing small  $E$  to be reached with tolerable (but still small!) time-steps. Significant advances have been made using this scheme (see, for example, Glatzmaier & Roberts 1995, 1997), but there is a serious price to pay. As pointed out by Zhang & Jones (1997), hyperdiffusion damps out small azimuthal wavenumbers, which can be preferred if the magnetic field is weak. To illustrate this we reproduce some of the Zhang & Jones (1997) results in figure 1*a–c*. In figure 1*a* we show the flow pattern at small  $E$  at the onset of non-magnetic convection; note the large preferred  $m$  visible from the tight roll configuration, and the largely  $z$ -independent nature of the flow expected from the Proudman–Taylor theorem. In figure 1*b* we see the result of the same calculation but with hyperviscosity and no magnetic field, while in figure 1*c* we see the equivalent picture for the case of an imposed azimuthal magnetic field and no hyperviscosity. Note that the hyperviscosity has produced a similar effect to the magnetic field, in both cases reducing the dominant azimuthal wavenumber. In consequence, it is very difficult to tell in dynamo simulations with hyperviscosity whether the azimuthal wavenumber is being determined by the magnetic field or the hyperviscosity. In this respect, the three-dimensional hyperdiffusive dynamos suffer from the same disadvantage as the  $2\frac{1}{2}$ -dimensional models in that the dominant azimuthal wavenumbers are selected somewhat arbitrarily.

Another approach is the use of finite differences in all three directions (see, for example, Kageyama & Sato 1997*a*). These methods became unfashionable because of difficulties in treating the flow near the rotation axis, and in implementing the correct magnetic boundary conditions, which are non-local. However, the development of fast massively parallel machines and the failure to resolve the Legendre transform problem (Lesur & Gubbins 1999) has stimulated new interest in finite-difference techniques, which can take full advantage of parallel architecture. The pseudo-spectral technique requires a redistribution of the arrays amongst the different processors at each time-step, and this makes it a less attractive scheme for parallel architecture.

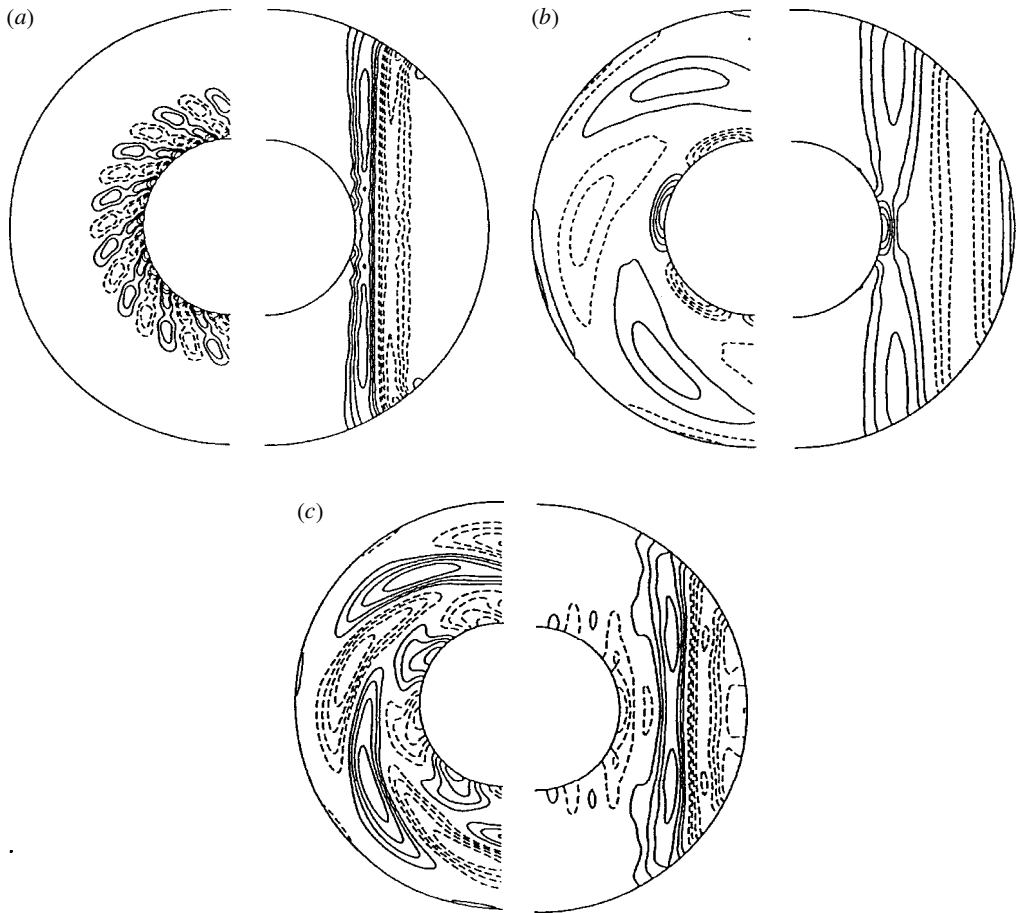


Figure 1. The pattern of convection with the preferred azimuthal wavenumber. On the right-hand side are contours of azimuthal velocity in a meridian plane; on the left-hand side are contours of azimuthal velocity in the equatorial plane: (a)  $E = 2 \times 10^{-5}$  with no magnetic field and no hyperviscosity; (b)  $E = 2 \times 10^{-5}$  with no magnetic field, but with hyperviscosity  $\lambda = 0.1$ ; (c)  $E = 2 \times 10^{-5}$  with no hyperviscosity but with magnetic field  $A = 1$ .

#### 4. Numerical results in the Busse–Zhang regime

The dimensionless parameter values for the Earth are rather extreme ( $E \sim 10^{-15}$  and  $q \sim 10^{-5}$ ; see also § 6), and no numerical simulation has even approached them. There is, however, one region of parameter space where solutions can be found with large, but not impossibly large, computing resources. This is the Busse–Zhang regime (Sarson *et al.* 1998), so called after the pioneering work of Busse (1976) and Zhang & Busse (1989) who first found solutions in this region of parameter space. Here dynamo action occurs at comparatively low Rayleigh number; typically a few times the critical value for the onset of convection itself. In this regime, the velocities are typically  $O(10)$  on the thermal diffusion time-scale. Since velocities have to be at least of order  $O(10^2)$  on the magnetic diffusion time-scale for dynamo action, i.e. the magnetic Reynolds number has to be  $O(10^2)$ , the value of  $q$  required for a successful

dynamo is  $O(10)$ . It is possible to obtain dynamo action at lower values of  $q$  by raising the Rayleigh number; in the range  $10R_c < R < 100R_c$  velocities are typically  $O(10^2)$  on the thermal time-scale, and then  $q \sim O(1)$  is sufficient for dynamo action. We call solutions at  $q \sim O(1)$  and large  $R$  Glatzmaier–Roberts dynamos. In principle, Busse–Zhang dynamos can occur over a wide range of Ekman numbers, down to very small values; in practice, numerical instability makes it virtually impossible to go below  $E \sim 10^{-4}$  without using hyperviscosity, and, as mentioned above, hyperviscosity does not allow us to capture the essential features of low Ekman number behaviour. Most published Busse–Zhang solutions therefore have  $E$  in the numerically accessible range  $10^{-4} < E < 10^{-3}$ . However, within this rather limited range of parameter space, a large number of calculations have been performed.

In addition to the pioneering papers of Busse and Zhang referred to above, recent fully three-dimensional simulations in this regime have been performed by Busse *et al.* (1998), Sakuraba & Kono (1999), Katayama *et al.* (1999), Kageyama & Sato (1997*a–c*), Kitauchi & Kida (1998), Kida & Kitauchi (1998*a,b*) and Olson *et al.* (1999) (see also Christensen *et al.* 1999). Fully  $2\frac{1}{2}$ -dimensional simulations in this regime have been performed by Jones *et al.* (1995), Sarson *et al.* (1997*a*, 1998) and Morrison & Fearn (2000).

Although the processes involved in convection-driven dynamos are very complex, there are fortunately many points of similarity emerging from all this activity, and some physical understanding of the basic processes is beginning to emerge. Figure 2 shows a snapshot of some results of a simulation with limited resolution in the  $\phi$  direction (modes  $m = 0, 2, 4, 6$  and  $8$  are present). In figure 2*a, b* a slice at constant  $z$  is shown (i.e. a plane parallel to the Equator), figure 2*a* showing the flow and figure 2*b* showing the magnetic field. The parameter values are  $R = 35$ ,  $q = 10$ ,  $E = 10^{-3}$  and  $Pr = \infty$ ; model details are as in Sarson *et al.* (1998). Figure 2*c* gives the corresponding axisymmetric fields plotted in a meridional slice. The pattern of convection found in this regime consists of columnar rolls which drift around in a prograde (eastward) direction. There is generally a small differential rotation, but not a differential rotation strong enough to produce a powerful  $\omega$ -effect;  $R$  is too low to generate a strong thermal wind; the flows are not large enough (unless  $Pr$  is small) for the nonlinear  $\mathbf{u} \cdot \nabla \mathbf{u}$  Reynolds stress terms to generate differential rotation, and the Lorentz force is not strong enough to drive substantial flows. In consequence, the dynamos are of the  $\alpha^2$ -type with toroidal and poloidal fields being generated locally in the convection rolls themselves (Olson *et al.* 1999). The toroidal and poloidal components of magnetic field are of broadly similar strength, and the magnetic field does not appear to have a very powerful effect on the convection in this regime. At  $E \sim 10^{-3}$  the dominant  $m$  is typically around 4, while at  $E \sim 10^{-4}$  the dominant  $m$  is in the range 6–8, depending on the model details, in particular the codensity source and the boundary conditions. Fixed flux boundary conditions, as used in the figure 2 calculations, generally favour lower values of  $m$ . The preferred number of rolls is usually close to that expected from linear non-magnetic convection at the same Ekman number (Christensen *et al.* 1999); this is, perhaps, slightly surprising as magnetoconvection studies indicate that lower values of  $m$  are preferred with imposed uniform magnetic fields when the Elsasser number is  $O(1)$ . However, the magnetic field in these solutions is very far from uniform and is strongly influenced by flux expulsion: it therefore appears that it is the convection which selects the wavenumber and the field responds to this choice.

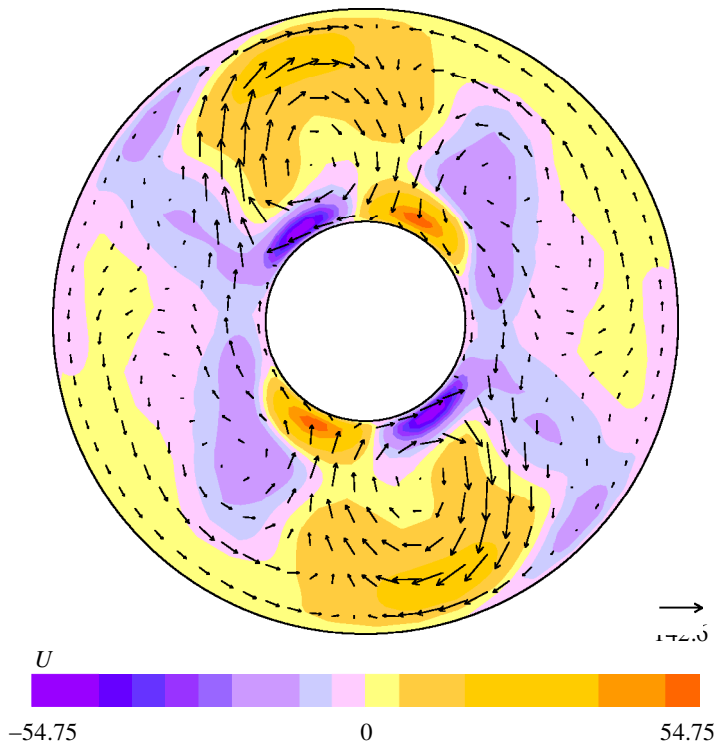


Figure 2. A snapshot of a solution in the Busse–Zhang regime,  $R = 35$ ,  $q = 10$ ,  $E = 10^{-3}$ . Azimuthal wavenumbers  $m = 0, 2, 4, 6, 8$  were present in the calculation. (a) The velocity field in the plane  $z = 0.15$  (where  $z = 0$  is the Equator and  $z = 1.5$  is the outer boundary North Pole; the plot is viewed from above) with imposed dipolar symmetry. The colours show the vertical velocity  $u_z$  (with colour intervals one-tenth of the maximum amplitude stated), the arrows the horizontal velocity  $u_h$  (the longest arrow corresponding to the maximum stated).

Hollerbach & Jones (1993) noted that the dynamical behaviour outside a cylinder enclosing the inner core (the tangent cylinder) was rather different from that of the polar regions inside the tangent cylinder. The two polar regions are usually fairly quiescent in the Busse–Zhang regime. Convection is more easily excited outside the tangent cylinder, where the convection rolls disturb the geostrophic constraint least. At mildly supercritical  $R$ , the polar regions are effectively convectively stable.

As noted by Busse (1976) the convection roll pattern is effective at generating magnetic field, and magnetic Reynolds numbers of  $O(100)$  are all that is needed. It is necessary to have motion along the rolls as well as around the rolls for dynamo action to occur. There are a number of possible sources for this, which contribute in different proportions according to the model details. The convection itself induces a  $z$ -velocity antisymmetric about the equatorial plane, which is significant in all the models. With no-slip boundaries, Ekman suction at the boundaries can also drive a  $z$ -velocity, thus enhancing the convective flow. Finally, if an inner core is present, the interaction of the rolls with the inner core near the tangent cylinder can generate  $z$ -velocity. Particularly in models where the driving is strongest near the inner core, this can be a powerful effect (see figure 2a).

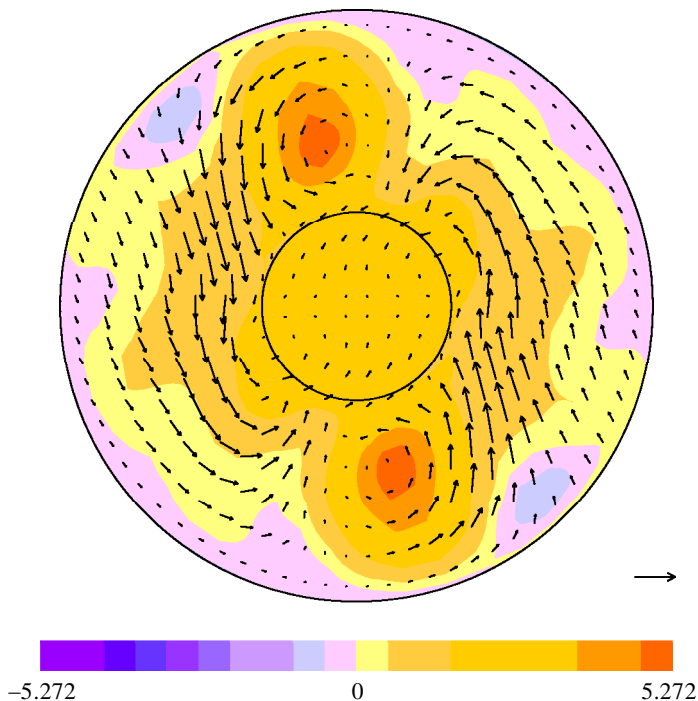


Figure 2. (*Cont.*) (*b*) As figure 2*a*, but for magnetic fields,  $B_z$  and  $B_h$ .

Although the magnetic field does not appear to have a striking effect on the flow, it must have some effect. Since the nonlinear advection term in the equation of motion does not play a very important role, the Lorentz force is the only significant nonlinear term. Furthermore, the induction equation is linear in  $\mathbf{B}$ , so the amplitude of the magnetic field can only be determined by the Lorentz force limiting the flow in some way. There appear to be a number of ways in which this limiting could take place. (i) In an  $\alpha\omega$  dynamo, generating field principally by a powerful differential rotation, the Lorentz force will act to brake the differential rotation and hence control the dynamo process. The amplitude of the field is then determined by the strength at which the forces producing differential rotation are sufficiently opposed by magnetic braking. However, this does not seem a likely mechanism in the Busse–Zhang regime, where differential rotation does not appear to be very important. A variation on this, which can apply also to  $\alpha^2$  models, is that the Lorentz force can generate a differential rotation which disrupts the dynamo process, thus bringing about equilibrium; the Malkus–Proctor scenario (Malkus & Proctor 1975). Although it might well be important at very low  $E$ , this mechanism does not seem to be very active in the numerical simulations. Another possibility, (ii), mentioned by Olson *et al.* (1999), is that the magnetic field directly reduces the convective velocity and hence reduces the magnetic Reynolds number to its critical value. In this mechanism, the magnetic braking acts not on the axisymmetric differential rotation, but on each individual roll. Possibility (iii) is that the magnetic field acts to reduce the stretching properties of the flow, i.e. magnetic field turns the generating process from an efficient dynamo into a less efficient dynamo. If this mechanism operates, the mean kinetic energy is not necessarily smaller with the saturated magnetic field than it is with zero field,

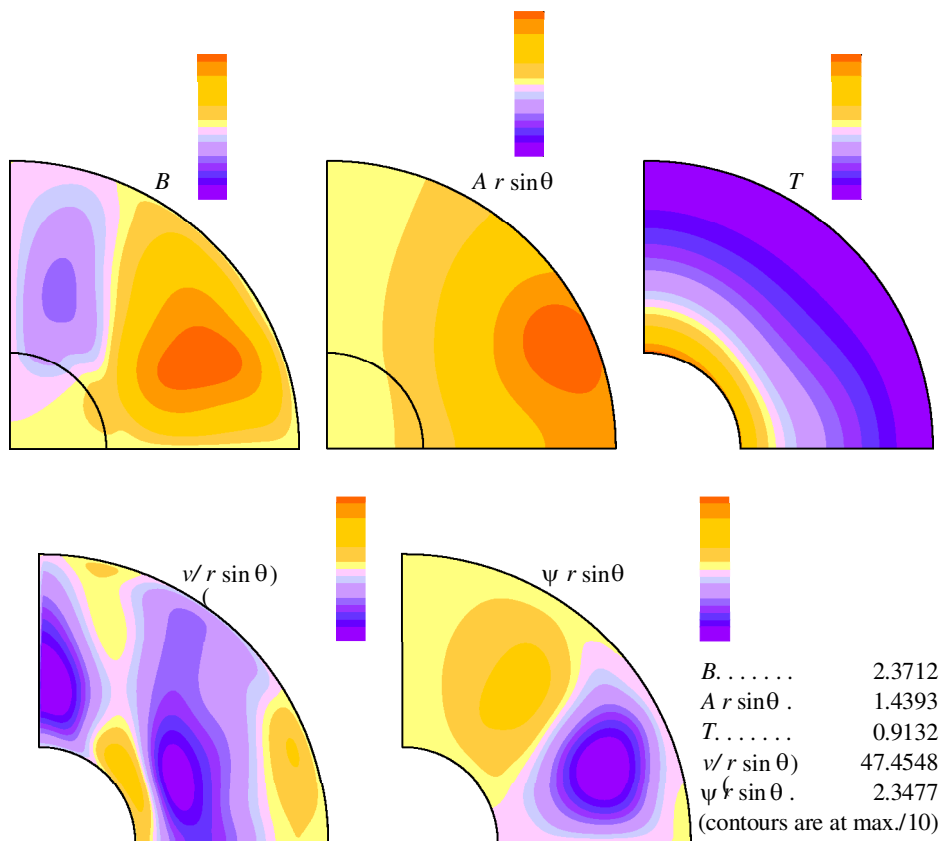


Figure 2. (*Cont.*) (*c*) A meridian slice of the axisymmetric components of various quantities:  $B$ , toroidal (zonal) magnetic field;  $A r \sin \theta$ , lines of force of poloidal (meridional) magnetic field;  $C$ , codensity;  $v/(r \sin \theta)$ , the azimuthal angular velocity;  $r \sin \theta$ , streamlines of the meridional circulation. Colour intervals are one-tenth of the maximum stated, with purple corresponding to negative values. In plots of zonal fields, positive contours denote eastward-directed fields. In plots of meridional quantities, the sense of field is clockwise around positive contours and anti-clockwise around negative contours.

and the nonlinear magnetic Reynolds number could be quite different in different parameter regimes. Since the stretching properties of a flow depend on rather subtle features involving derivatives of the velocities themselves, two flows which look superficially rather similar can have very different dynamo action properties. We should therefore perhaps not be too surprised that the convection in the magnetically saturated regime looks pretty similar to that in the zero-field regime. The differences are in the stretching properties of the field, which do not show up well in a simple velocity field plot. It is probably too early to say whether mechanism (ii) or (iii) is the most important in the Busse–Zhang regime, but we note from the data available that while there is some evidence that magnetic field reduces mean kinetic energy and hence typical velocities, the reduction is not generally very great, while there is a considerable variation in the magnetic Reynolds number of the saturated flow, suggesting mechanism (iii) may be the more important.

While the influences of the magnetic field on the flow are not generally large in this regime, as noted above, it is of interest to try to analyse those which do occur. Kagayama & Sato (1997*c*) noted that rolls can be divided into cyclonic and anticyclonic rolls, depending on whether the vorticity of the roll added to, or subtracted from, the planetary vorticity. Anticyclonic rolls have the  $z$ -velocity positive in the Northern Hemisphere and negative in the Southern Hemisphere. The  $z$ -velocity is therefore divergent near the Equator, and so by the continuity equation, the horizontal flow in an anticyclonic roll converges near the Equator. This horizontal converging flow tends to accumulate magnetic field near the centres of anticyclonic rolls in the equatorial region, but in cyclonic rolls the horizontal flow near the Equator is divergent, and so no field accumulates there. Note that in figure 2*b*, the vertical magnetic field is strongest in the two anticyclonic rolls (clockwise flow), so the magnetic field produces a strong asymmetry between cyclonic and anticyclonic rolls. Sakuraba & Kono (1999) note that the magnetic field in the centres of anticyclonic rolls tends to expand them, so they become larger than the cyclonic rolls (note that the anticyclonic vortices in figure 2*a* are indeed more pronounced than the cyclonic vortices). The average vorticity of the roll system is then negative, leading to westward flow near the CMB and eastward flow near the inner core.

## 5. Numerical results in the Glatzmaier–Roberts regime

The other regime that has been studied is the higher Rayleigh number regime, typically  $R \sim O(100R_c)$ . Since the velocities here are larger compared with the thermal diffusion time than in the Busse–Zhang regime, one can afford to reduce  $q$  to an  $O(1)$  value, and still have  $R_m$  large enough for dynamo action. Since at smaller values of  $E$  convection is more organized, reducing  $E$  allows larger  $R$  and so allows smaller  $q$ . Interestingly, increasing the Rayleigh number at fixed Ekman number can actually lead to a loss of dynamo action (Morrison & Fearn 2000; Christensen *et al.* 1999). The velocities may be larger, but the more disorganized flow is less efficient as a dynamo. Christensen *et al.* (1999) find empirically  $q_c \sim 450E^{3/4}$  as the minimum possible value of  $q$  for dynamo action on the basis of their numerical experiments.

Some of the larger  $R$  calculations have been done with hyperviscosity, so it is not easy to estimate the effective Ekman number in these cases. Nevertheless, the main features of these higher  $R$  dynamos have been found in a range of models and are probably robust.

In figure 3 we show the same constant  $z$  slice and meridional slice as in figure 2, but now the Rayleigh number is much larger and the Ekman and Roberts numbers are reduced by a factor of 10: the parameters are  $R = 45\,000$ ,  $E = 10^{-4}$ , but with some hyperdiffusivity, and  $q = 1$ . The most important feature is that the differential rotation  $v/r \sin \theta$  becomes much stronger in this regime (cf. figures 2*c* and 3*c*). The convection is more chaotic, and the rolls lose their clear-cut identity, typically lasting for only a short time. Nevertheless, the convection is highly efficient, in the sense that the temperature gradients are confined to thin boundary layers and the bulk of the region outside the tangent cylinder and outside of these boundary layers is nearly isothermal; note the much thinner boundary layers of  $C$  in figure 3*c* than in figure 2*c*. Because the surface area of the outer CMB boundary layer is so much greater than that of the ICB boundary, this isothermal region is at a temperature much closer to that of the CMB than the ICB, i.e. it is relatively cool. Convection

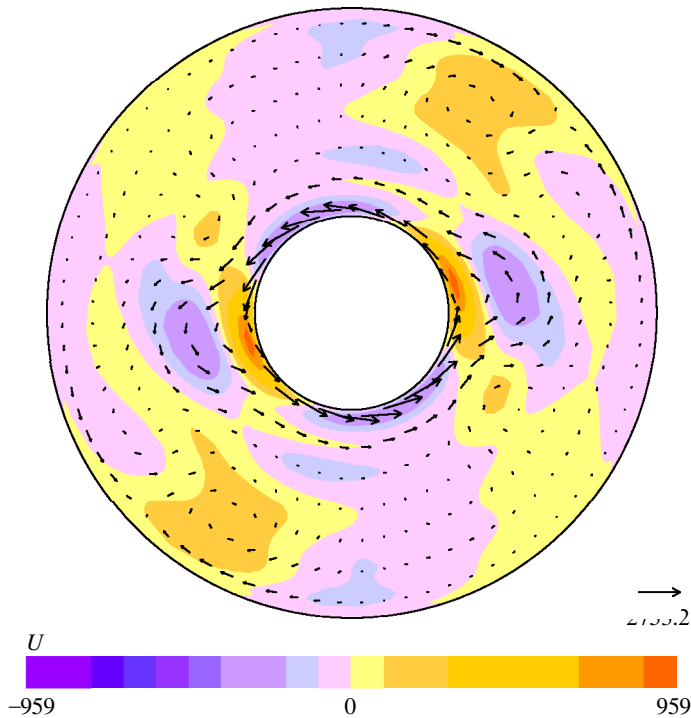


Figure 3. A snapshot of a solution in the Glatzmaier–Roberts regime,  $R = 45\,000$ ,  $q = 1$ ,  $E = 10^{-4}$  with hyperviscosity  $\lambda = 0.05$ . Azimuthal wavenumbers  $m = 0, 2, 4, 6, 8$  were present in the calculation. No symmetry about the Equator was imposed. (a)–(c) are as in figure 2.

also occurs now in the polar regions inside the tangent cylinder: here the geometry is such that the mean temperature of the fluid is closer to the average of the ICB and CMB temperatures, much hotter than that of the bulk of the fluid outside the tangent cylinder. In consequence, there are strong temperature gradients in the  $\theta$  direction, so that there is a thermal wind

$$\frac{\partial v}{\partial z} = \frac{qR}{r} \frac{\partial T}{\partial \theta}, \quad (5.1)$$

which is large since  $\partial T/\partial \theta$  is  $O(1)$  and  $R$  is large in this regime. In the Northern Hemisphere  $\partial T/\partial \theta$  must be negative, for the reasons given above, and so  $\partial v/\partial z$  is negative in the Northern Hemisphere, so there is a strong prograde (eastward) flow near the ICB. This flow is then coupled to the ICB itself by viscous and magnetic torques (Aurnou *et al.* 1996), and so the inner core has to rotate rapidly eastward in this regime if gravitational torques are neglected. The pattern of the differential rotation (see figure 3c) is a very constant feature of models in this regime, and it leads to the generation of strong toroidal fields in the regions of high shear near the ICB (see figure 3b). The helicity in this regime is produced mainly by the interaction of convection with the inner core, and so poloidal field also is strongest near the inner core. The Glatzmaier–Roberts regime dynamos are therefore more like  $\alpha\omega$  dynamos with differential rotation playing an important role in the production of toroidal field. It should be noted, however, that the peak poloidal field strength is not that much smaller than the peak toroidal field strength.

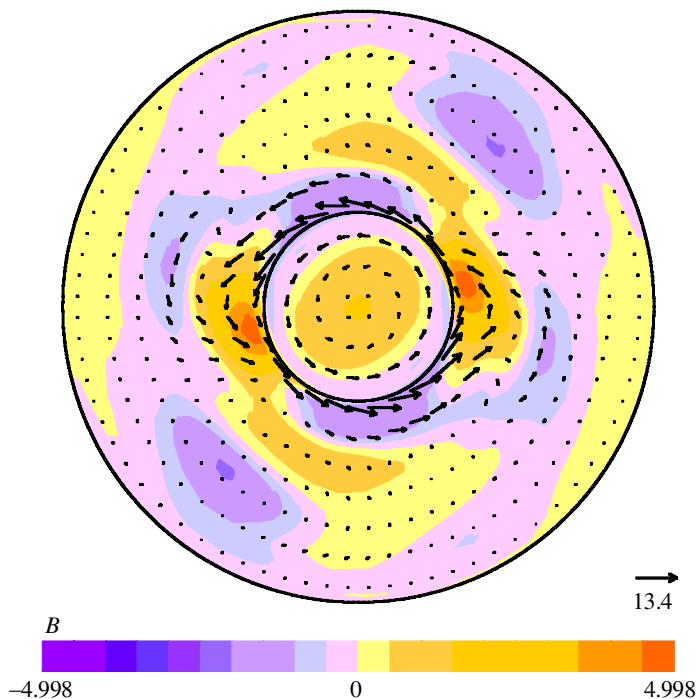


Figure 3. (Cont.) (b).

Another key difference from the Busse–Zhang model is that the polar regions inside the tangent cylinder are now very active, convecting vigorously and generating strong magnetic fields there. This polar convection changes the form of the codensity contours, which in turn change the form of the thermal wind, given by (5.1). The differential rotation in the Busse–Zhang models is therefore not only much weaker (because the thermal wind driving is proportional to  $R$ ) but has a different characteristic form (compare figure 2c with figure 3c). In the Busse–Zhang models the form of the differential rotation is such that there is no strongly preferred direction of rotation of the inner core, in contrast to the Glatzmaier–Roberts models.

Another characteristic feature of the Glatzmaier–Roberts regime is the presence of a strong axisymmetric meridional circulation ( $\psi r \sin \theta$  in figure 3c) in the polar regions inside the tangent cylinder. This circulation rises out from the ICB at the poles and falls back towards the ICB along the tangent cylinder. The flow returns from the tangent cylinder back to the poles along a thin Ekman boundary layer near the ICB, which controls the strength of the meridional circulation. A simple calculation of the Ekman-layer flow indicates that the strength of the meridional circulation as measured by the maximum value of  $\psi$  on the magnetic diffusion time-scale gives

$$\psi_{\max} \sim qRE^{1/2}.$$

This will be small in the Busse–Zhang regime, since there  $E$  is small and  $R$  is not large. In the Glatzmaier–Roberts regime,  $E$  cannot be made very small for stability reasons, but  $R$  is quite large, so a strong meridional circulation is found. This meridional circulation does not seem to be strongly affected by magnetic field in the regime

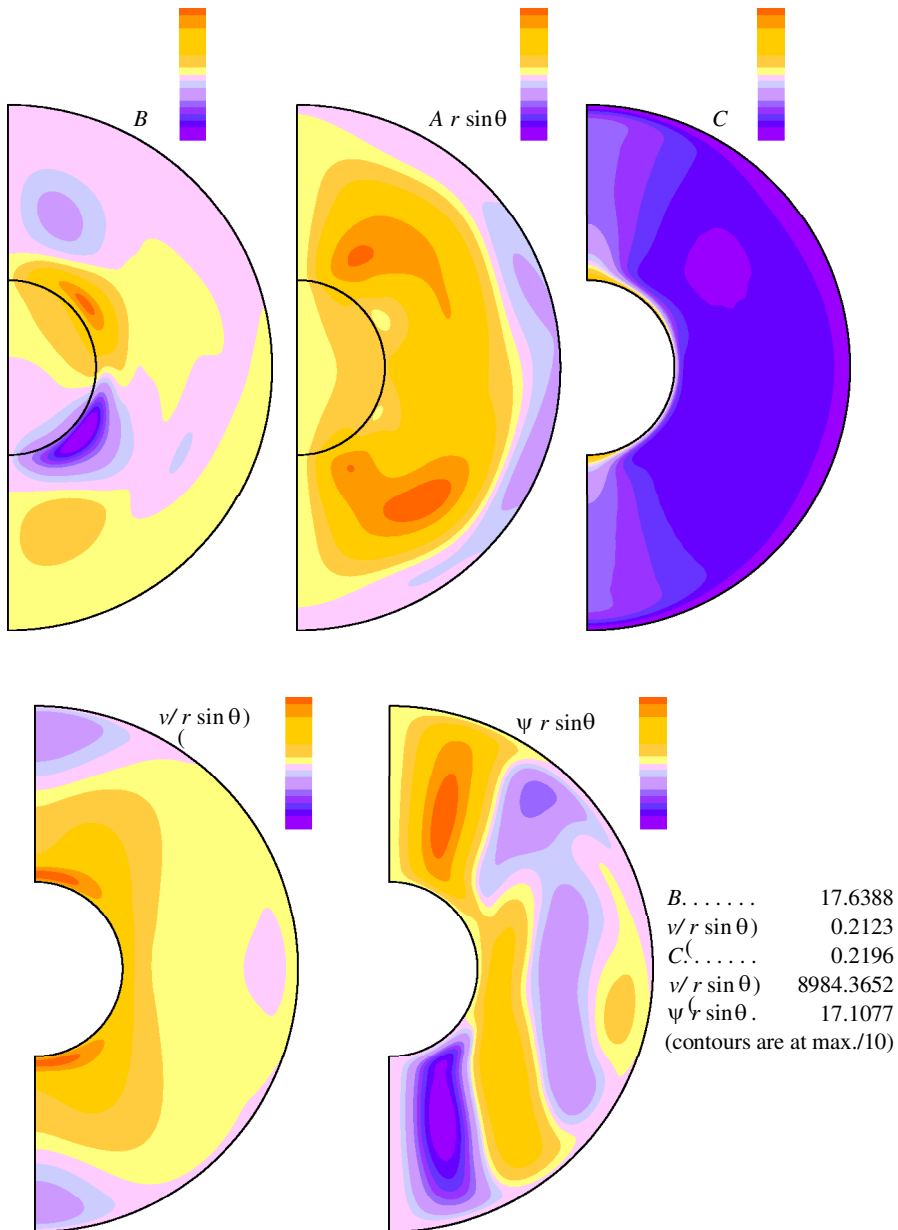


Figure 3. (Cont.) (c).

in which these models are run. Considerations such as these indicate how important it is to find out more about the parameter regime the geodynamo is operating in. Everyone knows that in the geodynamo  $R$  is large and  $E$  is small, but is the key parameter  $RE^{1/2}$  large, small or  $O(1)$ ? If the meridional circulation is significant, it may have very important consequences for the dynamo, in particular for the reversal mechanism (Sarson & Jones 1999; Glatzmaier *et al.* 1999).

## 6. The geodynamo parameter regime

Since it is clear that there are a number of different types of dynamo that can operate at low Ekman number, we need to consider the geophysical parameters carefully to see which types, if any, are connected with the geodynamo. It is also possible that qualitative differences occur between the behaviour at the moderately small Ekman numbers used in the simulations and the extremely low Ekman number found in the Earth's core.

Although it is likely that turbulence plays an important part in core dynamics (Braginsky & Meytlis 1990), we start by considering the parameter values based on molecular values (see, for example, Braginsky & Roberts 1995). We take the magnetic diffusivity of the core as  $\eta \sim 2 \text{ m}^2 \text{ s}^{-1}$ , which is equivalent to a conductivity of  $4 \times 10^5 \text{ S m}^{-1}$ . The thermal diffusivity is  $\kappa \sim 10^{-5} \text{ m}^2 \text{ s}^{-1}$  and the viscous diffusivity is near  $\nu \sim 10^{-6} \text{ m}^2 \text{ s}^{-1}$  (DeWijns *et al.* 1998). Based on these molecular diffusivities,  $q \sim 5 \times 10^{-5}$  and  $Pr \sim 0.1$ . The situation is complicated further because in the core thermal convection is not the only driving mechanism; compositional convection can occur, and may indeed be more important. The molecular value of the material diffusivity of light material in the core is even smaller,  $\kappa_\xi \sim 10^{-8} \text{ m}^2 \text{ s}^{-1}$ . The equation governing the concentration of light material, the codensity equation (2.3), is the same as the temperature equation, but the appropriate boundary conditions are different. The radius of the outer core is  $r_o = 3.48 \times 10^6 \text{ m}$ , the radius of the inner core  $r_i = 1.22 \times 10^6 \text{ m}$  and  $\Omega_0 = 7.3 \times 10^{-5} \text{ s}^{-1}$ . The molecular value of the Ekman number is then  $10^{-15}$ .

Estimating the molecular value of the Rayleigh number is more difficult; there are two Rayleigh numbers to consider, one for the thermal part of the convection and one for the compositional part. We consider the thermal Rayleigh number first. Since it is the heat flux which is fixed by mantle convection, the problem is slightly different from the classical Rayleigh–Bénard problem. A further difficulty is that the heat flux coming out of the core is not well known. This heat flux can be divided into two parts, that carried by conduction down the adiabatic gradient and that carried by convection down the superadiabatic gradient. It is only the convective part that is of relevance to driving the outer core; this total convective heat flowing out of the core is unlikely to exceed *ca.*  $5 \times 10^{12} \text{ W}$ , and we use this as our estimate for  $F_{\text{conv}} \sim 3 \times 10^{-2} \text{ W m}^{-2}$  at the CMB. It is possible that most of the heat flux is carried down the adiabatic gradient by conduction, and  $F_{\text{conv}}$  is much lower than this (Nusselt number close to unity).

A flux Rayleigh number can be defined by evaluating the (notional) superadiabatic temperature gradient that would be required to carry this convective part of the heat flux out by conduction, giving

$$Ra_f = \frac{g\alpha d^4 F_{\text{conv}}}{\kappa^2 \nu \rho c_p} \sim 10^{29}$$

taking  $\rho \sim 10^4 \text{ kg m}^{-3}$ ,  $c_p \sim 8 \times 10^2 \text{ J kg}^{-1} \text{ K}^{-1}$ ,  $\alpha \sim 10^{-5} \text{ K}^{-1}$  and  $g \sim 10 \text{ m s}^{-2}$  (Braginsky & Roberts 1995). The corresponding modified flux Rayleigh number is

$$R_f = \frac{g\alpha d^2 F_{\text{conv}}}{2\kappa^2 \Omega \rho c_p} \sim 10^{14}.$$

The flux Rayleigh number is appropriate for considering the onset of convection, but in strongly supercritical convection the superadiabatic temperature gradient will be

greatly reduced from the value

$$\beta = \frac{F_{\text{conv}}}{\kappa \rho c_p},$$

which it has near onset. In Rayleigh–Bénard convection the main effect of increasing  $Ra$  is to increase the heat flux for a given temperature difference between the boundaries; in fixed flux convection the main effect is to decrease the temperature difference for a given heat flux. If we want to use the results of Rayleigh–Bénard convection at fixed temperature (where there has been more previous work), it is more appropriate to estimate the Rayleigh number by estimating the typical temperature fluctuation and using this as an estimate of the superadiabatic temperature difference between the ICB and CMB,  $\Delta T$ . The convective heat flux is

$$F_{\text{conv}} = \int_S \rho c_p u_r T \, ds. \quad (6.1)$$

We must assume that the integral (6.1) can be approximated by taking typical values of  $u_r$  and  $\Delta T$ ; this assumes that the radial velocity and temperature fluctuations are well correlated, but we would expect this in a convection-driven fluid. We must also assume that the temperature variations are fairly uniform across the interior of the fluid outer core, and not concentrated into thin plumes. In the neighbourhood of the inner core we then estimate

$$4\pi r_i^2 \rho c_p u_r \Delta T \sim 5 \times 10^{12} \text{ W} \quad (6.2)$$

and then  $\Delta T \sim 10^{-4}$  K, slightly less than the estimate of  $\Delta T \sim 10^{-3}$  K of Braginsky & Roberts (1995). This seems a tiny temperature difference compared with the actual temperature difference between the ICB and CMB (*ca.* 1300 K), but it reflects the fact that very large convected heat fluxes can be carried by very small superadiabatic gradients, just as they are in stars. A similar estimate for  $\Delta T$  can be obtained by assuming that the magnitude of the buoyancy  $g\alpha\Delta T$  is similar to the magnitude of the Coriolis force  $2\Omega_0 u$  with  $u$  again estimated at  $3 \times 10^{-4} \text{ m}^2 \text{ s}^{-1}$ .

The modified Bénard Rayleigh number is then

$$R_B = \frac{g\alpha\Delta T d}{2\Omega\kappa} \sim 1.5 \times 10^7.$$

The non-rotating Rayleigh number is

$$Ra_B = R/E \sim 1.5 \times 10^{22}.$$

The Rayleigh number for compositional convection can be evaluated in a similar way, provided the mass flux is assumed, which is more or less equivalent to assuming the age of the inner core is known. Taking the density difference between the inner and outer core as  $0.6 \times 10^3 \text{ kg m}^{-3}$  and assuming the rate of growth of the inner core has been constant over the last  $4.5 \times 10^9$  years, then the rate of mass increase inside a sphere of fixed radius  $r > r_i$  is  $3.2 \times 10^4 \text{ kg s}^{-1}$ . Assuming most of this mass flux is carried out by advection rather than diffusion, then

$$3.2 \times 10^4 \text{ kg s}^{-1} \sim \int_S C u_r \, ds$$

from (2.3). Again taking  $\Delta C$  as the typical difference in  $C$  between upward and downward moving fluid gives  $\Delta C \sim 5 \times 10^{-6} \text{ kg m}^{-3}$ , giving the modified Rayleigh number  $R_B = g\Delta C d / 2\rho\Omega_0\kappa\xi \sim 10^{10}$ ; the fact that the compositional Rayleigh number is larger than the thermal Rayleigh number is due to  $\kappa\xi$  being considerably smaller than  $\kappa$ .

(a) *The dynamo catastrophe*

A number of attempts to achieve a low-Ekman-number convection-driven dynamo using the magnetostrophic equations in the interior together with Ekman boundary layers have been made. All have so far failed, due to what might be termed the ‘dynamo catastrophe’.

The attempts all started with the idea that convection at low Ekman number but  $O(1)$  Elsasser number need not occur on the very small azimuthal and radial length-scales that occur in the non-magnetic problem. Indeed,  $O(1)$  length-scales are the preferred linear mode when there is an imposed (axisymmetric) magnetic field. Since large-scale convection has been found in all simulations to give rise to dynamo action, the hope was that the large-scale convection could generate the large-scale field required and hence maintain a self-consistent large-scale dynamo. The problem with this scenario is that the magnetic field needs to be sufficiently strong everywhere and at all times to sustain convection on a large length-scale (Zhang & Gubbins 2000). If, due to fluctuations, the field becomes small over a significant domain for a significant period (e.g. at a reversal), the length-scale of convection becomes short, and the dynamo fails. The magnetic field then starts to decay, and so small-scale convection takes over everywhere, permanently. A dynamo catastrophe has occurred, and the field can never recover.

We might ask why the simulations referred to above do not show this catastrophic failure. The simulations that have been performed to date have not been in the regime where the magnetic field is playing a major role in selecting the preferred wavenumber: indeed, as remarked above, in most simulations the preferred azimuthal wavenumber is not very different to that expected with non-magnetic linear convection. None of the simulations have yet reached the very low Ekman regime where the dynamo catastrophe occurs.

The dynamo catastrophe can be understood in terms of the various bifurcations that occur in convection-driven dynamos. As the Rayleigh number is increased, there may be various non-magnetic bifurcations in the convective flow, but eventually, at large enough magnetic Reynolds number, there is likely to be a critical value of the Rayleigh number  $R_c$  at which dynamo action occurs; this bifurcation may be supercritical or subcritical. If it is supercritical, then a finite-amplitude magnetic-field state is established for values of  $R > R_c$ . This state is generally known as the weak-field dynamo regime (see, for example, Roberts & Soward 1992) and is characterized by the small wavelengths in the direction perpendicular to the rotation axis. This state was analysed in the plane layer dynamo case by Childress & Soward (1972). They found that the weak-field regime only existed for a fairly restricted range of Rayleigh number, because the magnetic field enhanced convection, eventually leading to runaway growth; the weak-field regime therefore terminates at some  $R_{\text{rway}}$ , so the weak-field regime only exists for  $R_c < R < R_{\text{rway}}$ . Childress & Soward (1972) conjectured that a subcritical branch of strong-field solutions also exists, with

wavenumbers of  $O(1)$  and with magnetic-field strength such that the Elsasser number is  $O(1)$ , and that when  $R > R_{\text{rway}}$  the solution jumps onto this branch. This strong-field regime is likely to exist for Rayleigh numbers much less even than  $R_c$ , although for the numerical reasons given above this has not yet been unambiguously demonstrated. If the Rayleigh number is decreased on the strong-field branch, there must come a point at which the magnetic Reynolds number is too small to support dynamo action, say  $R = R_s$ , and below this no magnetic field can be sustained. The dynamo catastrophe arises when  $R_s \ll R_c$ , the likely situation in the geodynamo, and when the actual Rayleigh number is in the range  $R_s < R < R_c$ ; ‘safe’ dynamos are those where  $R > R_c$ .

In subcritical dynamos there are at least two stable attracting states, one with magnetic field and one without. In most of the simulations, the state with the magnetic field is chaotic, so it is subject to considerable fluctuation. It is possible to wander on a chaotic attractor without ever falling into an attracting fixed point; an example is the Lorentz attractor, where for some parameter values there are two attracting fixed points, but some solutions wind around these attracting fixed points without ever falling into their basin of attraction. The geodynamo could perhaps behave in a similar fashion, though other planets which no longer have internal dynamos may have suffered a dynamo catastrophe in the past. Another issue that arises with subcritical models of the geodynamo is how the magnetic field started in the first place; convection can only occur in a core at a temperature well above the Curie point; even if the geodynamo is currently subcritical, it must have been supercritical some time in its past.

It is of interest to estimate the parameter regime where we expect the dynamo catastrophe to occur, and conversely to find where ‘safe’ (supercritical) dynamos, i.e. those where magnetic field can be regenerated from the non-magnetic convecting state, are located. At Prandtl numbers of  $O(1)$ , non-magnetic convection in a rapidly rotating sphere has a preferred azimuthal wavenumber  $m \sim E^{-1/3}$ , and a similar radial length-scale. The planform will therefore be of convection roll type, not dissimilar to that found in the Busse–Zhang models, but with a much smaller radial and azimuthal length-scale.

Since the asymptotic theory of linear convection in a rapidly rotating sphere (or spherical shell) at small  $E$  has now been worked out (Jones *et al.* 2000), at least in the case of uniform heating, we can apply this theory to see what kind of convection we expect at these extreme parameter values. At  $Pr = 0.1$  the critical modified Rayleigh number for a radius ratio of 0.35 is  $0.27 \times E^{-1/3}$ , which is  $R_c = 2.7 \times 10^4$  at  $E = 10^{-15}$ . The thermal Rayleigh number is therefore supercritical,  $R/R_c \sim 500$ , but perhaps surprisingly not enormously so. The critical azimuthal wavenumber is  $m = 0.24E^{-1/3}$  which gives  $m \sim 2.4 \times 10^4$ . If this many rolls have to fit into the Earth’s core, each roll would have a diameter of *ca.* 0.4 km. Linear theory shows that at onset the rolls only occur at a specific distance (about  $0.7r_0$ ) from the rotation axis, but fully nonlinear convection rolls would probably fill the whole fluid core.

(b) *The minimum roll size for dynamo action*

If we (temporarily) accept that nonlinear non-magnetic convection in the rapidly rotating spherical shell takes the form of rolls of typical diameter somewhat less than 1 km with typical velocity  $u \sim 3 \times 10^{-4} \text{ m}^2 \text{ s}^{-1}$ , could this flow be a dynamo? The

kinematic dynamo problem for a related type of flow,

$$\mathbf{u} = \left( \sqrt{2} \sin \frac{\pi x}{a} \cos \frac{\pi y}{a}, -\sqrt{2} \cos \frac{\pi x}{a} \sin \frac{\pi y}{a}, 2 \sin \frac{\pi x}{a} \sin \frac{\pi y}{a} \right), \quad (6.3)$$

has recently been considered by Tilgner (1997). The flow has the form (6.3) inside a cylinder of height and radius  $R$ , and is zero outside it. The diameter of each roll is  $a$ , so that  $a$  is approximately  $2R/N$ , where  $N$  is the number of rolls that fit across the diameter of the cylinder. The length-scale for the flow is now  $a$ , so the local magnetic Reynolds number is  $R_m^o = ua/\eta$ . If the mean field strength is  $B$ , the fluctuations produced by the flow will be  $b^o \sim R_m^o B$ . The large-scale EMF is then  $\overline{\mathbf{u} \times \mathbf{b}^o}$ , which will maintain the current on the long length-scale  $d$  provided  $R_m^o u \sim \eta/d$ , or more precisely

$$R_m^o R_m = (a/d) R_m^2 > R_{mc}^2 \quad (6.4)$$

for some critical  $R_{mc}$ . If  $d$  and  $\eta$  remain fixed, as  $a/d$  decreases,  $R_m$  must increase as  $R_m \sim (a/d)^{-1/2}$  to maintain dynamo action. Tilgner (1997) finds that with a lattice of size  $N = 8$  rolls across a diameter,  $R_m$  must exceed  $R_{mc} \sim 15$ , and that for larger  $N$ ,  $R_{mc}$  increases as  $N^{1/2}$ , as expected from (6.4). We therefore have from Tilgner's calculation that  $R_{mc} \sim 15(N/8)^{1/2}$ .  $N$  cells across a diameter will correspond roughly to  $\pi N$  cells round the circumference, and so for convecting rolls with azimuthal wavenumber  $m$ ,  $m \sim \frac{1}{2}\pi N$ , giving  $R_{mc} \sim 7m^{1/2}$  for large  $m$ . It should be noted that the velocity field here is independent of  $z$ ; in convecting rolls,  $u_z$  is antisymmetric in  $z$ , and the dynamo will be less efficient. Data from the dynamo calculations of Christensen *et al.* (1999) suggest that the critical magnetic Reynolds number is at least a factor of three greater in convection cells than in the Tilgner cells, so we estimate

$$R_{mc} \sim 20m^{1/2}, \quad m \text{ large} \quad (6.5)$$

as the critical magnetic Reynolds number at large azimuthal wavenumber. Note that we are assuming here that the Rayleigh number is large enough for the convection rolls to effectively fill most of the outer core for this estimate. Taking  $3 \times 10^{-4} \text{ m s}^{-1}$  as our standard velocity for the core, and  $\eta = 2 \text{ m}^2 \text{ s}^{-1}$  for the magnetic diffusivity,  $R_m \sim 500$  for the Earth's core. Using our estimate (6.5) we then get  $m \sim 600$  as the maximum possible value of  $m$  at which we can expect dynamo action. Although this is a large value of  $m$ , it is a lot less than the value expected at  $E \sim 10^{-15}$ , which was  $m \sim 24\,000$ . The value of  $E$  at which  $m = 600$  is preferred at  $Pr = 0.1$  is around  $6 \times 10^{-11}$ .

The outcome of our estimates is therefore that 'safe' (supercritical) geodynamos could exist at Ekman numbers down to about  $E \sim 10^{-10}$ , but at Ekman numbers below  $10^{-10}$ , the preferred roll size for non-magnetic convection is too small to give a viable dynamo. For Ekman numbers below  $E \sim 10^{-10}$ , the dynamo must be sub-critical.

### (c) Convective velocities

So far our estimates have all been based on the value of  $3 \times 10^{-4} \text{ m s}^{-1}$  for the convective velocity. Would convection in this parameter regime actually give rise

to velocities of  $3 \times 10^{-4} \text{ m s}^{-1}$ ? If our underlying physical assumptions are correct, then the answer has to be yes, or else our picture is not self-consistent. It might be argued that we already know the answer is yes, because the velocities coming out of the simulations are of the right order of magnitude: the Busse–Zhang regime velocities are perhaps a little low, and the Glatzmaier–Roberts regime velocities a little high, but given the uncertainties involved in estimating  $\eta$  and in interpreting secular variation data to estimate  $u$ , this is not a cause for concern. However, this really begs the question, because the simulations assume turbulent values of the thermal, compositional and viscous diffusion which are tuned to give the right answers.

The usual velocity scale for mildly supercritical convection is the thermal velocity scale  $\kappa/d \sim 3 \times 10^{-12} \text{ m s}^{-1}$ , eight orders of magnitude too small. The velocity scale for compositional convection is a further three orders smaller. Clearly, for a convection-based geodynamo theory to work, we have to explain why the observed velocities are so large compared with the thermal velocity scale. Weakly nonlinear theory suggests that the velocities scale with  $(R/R_c)^{1/2}$ , and Zhang (1991) gives

$$u \sim 25[(R - R_c)/R_c]^{1/2} \kappa/d$$

for infinite Prandtl number convection. With the Bénard estimates for  $R$  and  $R_c$ , the expected velocity goes up to  $2 \times 10^{-9} \text{ m s}^{-1}$ , still far too small. Using compositional convection estimates reduces the expected velocity.

One possibility is that the magnetic field enhances the velocity, but even if the critical Rayleigh number is reduced from  $\sim 10^4$  down to unity by magnetic field, the Zhang formula still gives velocities three orders of magnitude too small. We need an improvement on weakly nonlinear theory to reach velocities as large as  $10^{-4} \text{ m s}^{-1}$ .

Unfortunately, not much is known about nonlinear convection at very low Ekman number. Probably the best available theory is that of Bassom & Zhang (1994), which is, however, based on non-magnetic Boussinesq convection in a plane layer, not with spherical geometry. Ignoring some logarithmic terms of the Rayleigh number, they give the vertical velocity for Rayleigh numbers well above critical as

$$u_z \sim 0.3R\kappa/d, \quad (6.6)$$

which gives  $u_z \sim 10^{-5} \text{ m s}^{-1}$ , which is getting closer to the required velocity. Considerable caution is needed in interpreting this result, though, because not only could the spherical geometry make a significant difference, at large  $R$  the flow will almost certainly be unstable, and this may reduce the velocities achieved. Nevertheless, it does suggest that because of the unusual nonlinear dynamics of rapidly rotating flows, the very large velocities (in terms of the thermal diffusion velocity scale) might be explicable. It is perhaps worth noting that the Bassom–Zhang theory gives an unusually strong dependence of typical velocity and Nusselt number on Rayleigh number with  $u \sim R$  and  $Nu \sim R$  (again ignoring logarithmic terms). Weakly nonlinear theory gives only  $u \sim R^{1/2}$  as mentioned above. Boundary-layer theories of non-rotating non-magnetic convection have dependencies which are affected by the precise nature of the boundary conditions, but Nusselt number  $Nu \sim R^{1/3}$  and  $u \sim R^{2/3}$  are perhaps typical.

(d) *The effect of turbulence in the core*

If our understanding of the effect of magnetic fields on strongly nonlinear low- $E$  convection is limited, the situation as regards turbulence in the core is even more

uncertain. Stevenson (1979) and Braginsky & Meytlis (1990) have considered the problem, and made tentative mainly qualitative estimates of the effect of turbulence. It is generally believed that turbulence is important in the Earth's core and will enhance the diffusive processes. This can significantly affect behaviour; for example, if turbulent diffusion can enhance the effective value of  $E$  to greater than  $10^{-10}$  the dynamo could be changed from subcritical to supercritical. Unfortunately, as stressed by Braginsky & Meytlis (1990) and Braginsky & Roberts (1995), turbulence in the extreme conditions in the core is quite unlike 'normal' turbulence. In normal turbulence, the nonlinear advection terms  $\mathbf{u} \cdot \nabla \mathbf{u}$  in the momentum equation play a key role; but these terms are small in the Earth's core. High Prandtl number Bénard convection at large Rayleigh number is an example of a system which shares this property and is well studied; the analogy is imperfect, though, because in the core Coriolis and Lorentz forces will give rise to strong anisotropy absent in high- $Pr$  convection.

Braginsky & Meytlis (1990) consider turbulence generated by local convection with strong rotation and azimuthal magnetic field. They note that the fastest growing modes are plate-like cells, with the short radial length-scale expected from non-magnetic convection, but with the azimuthal length-scale increased by the azimuthal magnetic field. The duration of the cells is assumed to be the growth rate of the convective instability, *ca.*  $6 \text{ yr}^{-1}$ , and their size in the azimuthal and  $z$ -directions is then determined to be *ca.* 50 km from the usual estimate of the velocity. The radial length-scale is much smaller at *ca.* 2 km. The resulting turbulent diffusivities are then *ca.*  $1 \text{ m}^2 \text{ s}^{-1}$  in the azimuthal and  $z$ -directions, and much smaller in the radial direction. The axis of the plate-like cells will be in the direction perpendicular to the rotation axis and the magnetic field, so unless the azimuthal field dominates other components, the anisotropic diffusion tensor will be a strong function of position.

Another difficulty is that a local theory, such as the Braginsky–Meytlis theory, is unlikely to be valid near the ICB and the CMB; but it is the boundary layers that control high Rayleigh number convection.

#### (e) Taylor's constraint

Taylor (1963) observed that if the magnetic field in the Earth's core was in magnetostrophic balance (Coriolis, Lorentz and pressure forces, with viscous and inertial forces negligible), the magnetic field has to satisfy the constraint

$$\int_S (\mathbf{j} \times \mathbf{B})_\phi \, dS = 0, \quad (6.7)$$

where  $S$  is any cylinder concentric with the rotation axis. A large literature has developed concerning nonlinear  $\alpha$ - $\omega$  dynamo models, and whether or not they satisfy Taylor's constraint, recently reviewed by Fearn (1998). It is natural to enquire whether the convection-driven geodynamo models satisfy Taylor's constraint. Sarson & Jones (1999) analysed dynamos in the Glatzmaier–Roberts regime, with low headline  $E$  but with hyperviscosity. They found that Taylor's constraint was not well satisfied, suggesting that viscous effects are playing an important part in these models. This is not perhaps surprising, as we know the current generation of dynamo models is still viscously controlled rather than magnetically controlled. As  $E$  is reduced from the currently available values of  $10^{-4}$ , initially we expect the roll diameter to

decrease so that viscous forces can still control the convection, and the magnetic-field scale to decrease similarly. These small-scale fields need not obey Taylor's constraint, since on that scale Lorentz forces can be balanced by viscous forces. However, as  $E$  reduces further, magnetic diffusion will prevent the magnetic-field scales getting smaller, while viscous forces can only be significant on very small length-scales unless large velocities occur. At these values of  $E$ , which are considerably smaller than those currently attainable, the dynamo must choose between satisfying Taylor's constraint (the Malkus–Proctor scenario) or maintaining a high-velocity zonal wind with which viscosity acting through the Ekman boundary layer can balance the Lorentz torque (Braginsky's model-Z scenario). The current generation of models has not yet reached  $E$  sufficiently small to give any indication into which of these two scenarios convection-driven dynamos will jump.

## 7. Conclusions

The current generation of numerical dynamos has been remarkably successful in bringing theoretical dynamo models into contact with geophysical reality. As a result of a concerted international effort, we are beginning to understand the physical mechanisms operating in these models, so that we can analyse why they behave as they do. We are also beginning to understand how the models vary as functions of the parameters, within the numerically accessible range. Fundamentally different regimes are found depending on how large the Rayleigh number is compared with the Ekman number. As computer technology advances there is every prospect that our understanding of the behaviour at moderate  $R$  and  $E$  will be enhanced.

It is clear, however, that the parameter regime operating in the Earth is far beyond that which can be simulated directly. The only way open to us to bridge the gap in the parameter space is by developing our understanding of the physical processes further, so that we can work out the asymptotic laws that govern these processes and hence extrapolate to the geophysical parameter range. At present, we do not know enough about the basic dynamics of rapidly rotating convection in spherical geometry in the presence of magnetic field for this to be possible. Some of the key questions we would like to answer are as follows.

- (i) What is the dominant length-scale of convection rolls in the core? Is the dominant transverse length-scale of the order of the core radius, with perhaps  $m = 2$  as suggested by some magnetic observations (Gubbins & Bloxham 1987), secular variation studies (Bloxham & Jackson 1991) and with some theoretical support (Longbottom *et al.* 1995); or is the transverse length-scale much smaller? The current models show very little evidence of the magnetic field increasing the transverse length-scales above those predicted by non-magnetic low- $E$  convection, so maybe the strongly non-axisymmetric magnetic field plays a more subtle role in the pattern selection process than is at present understood.

From our studies, we have a minimum roll diameter of *ca.* 15 km below which a dynamo cannot operate; the actual roll diameter cannot be too small, or else Ohmic dissipation would be too large, but we still have a large range of uncertainty. Unfortunately, small-scale magnetic fields at the CMB cannot easily be detected at the Earth's surface, because their influence declines rapidly with distance.

- (ii) How do the smaller scales of motion interact with the larger scales? In particular, if the effective eddy diffusivity is anisotropic, how will that affect the large-scale behaviour? A related question is what is the nature of the thermal and compositional boundary layers, and do they control the convection?
- (iii) What is the effect of the magnetic field on the convection? The current models show only a rather weak effect, less than would have been expected on the basis of magnetoconvection calculations with axisymmetric fields. However, it is hard to believe that the field will not have a major impact at low  $E$ ; the question is perhaps when it kicks in.

These questions will not be easy to answer, but with a combination of process studies of low  $E$  magnetoconvection, laboratory experiments and detailed comparison of dynamo simulation outputs with geophysical observation hopefully progress will be made.

I thank Dr Graeme Sarson for many discussions, and in particular for computing the solutions shown in figures 2 and 3, and Professor K. Zhang for computing the solutions shown in figure 1, and for many discussions in which our ideas about the geodynamo emerged. This work was supported by the UK PPARC grant GR/K06495.

## References

- Aurnou, J., Brito, D. & Olson, P. 1996 Mechanics of inner core super-rotation. *Geophys. Res. Lett.* **23**, 3401–3404.
- Bassom, A. P. & Zhang, K. 1994 Strongly nonlinear convection cells in a rapidly rotating fluid layer. *Geophys. Astrophys. Fluid Dynam.* **76**, 223–238.
- Bloxham, J. & Jackson, A. 1991 Fluid flow near the surface of the Earth's outer core. *Rev. Geophys.* **29**, 97–120.
- Braginsky, S. I. 1994 The nonlinear dynamo and model-Z. *Lectures on solar and planetary dynamos* (ed. M. R. E. Proctor & A. D. Gilbert), pp. 267–304. Cambridge University Press.
- Braginsky, S. I. & Meytlis, V. P. 1990 Local turbulence in the Earth's core. *Geophys. Astrophys. Fluid Dynam.* **55**, 71–87.
- Braginsky, S. I. & Roberts, P. H. 1995 Equations governing convection in Earth's core and the geodynamo. *Geophys. Astrophys. Fluid Dyn.* **79**, 1–97.
- Buffett, B. A. 1997 Geodynamic estimates of the viscosity of the Earth's inner core. *Nature* **388**, 571–573.
- Busse, F. H. 1976 Generation of planetary magnetism by convection. *Phys. Earth Planet. Interiors* **11**, 241–268.
- Busse, F. H., Grote, E. & Tilgner, A. 1998 On convection driven dynamos in rotating spherical shells. *Studia Geoph. Geod.* **42**, 1–6.
- Childress, S. & Soward, A. M. 1972 Convection driven hydromagnetic dynamo. *Phys. Rev. Lett.* **29**, 837–839.
- Christensen, U., Olson, P. & Glatzmaier, G. A. 1999 Numerical modelling of the geodynamo: a systematic parameter study. *Geophys. J. Int.* **138**, 393–409.
- Cox, S. M. & Matthews, P. C. 1997 A pseudo-spectral code for convection with an analytical/numerical implementation of horizontal boundary conditions. *Int. J. Numer. Meth. Fluids* **25**, 151–166.
- DeWijns, G. A., Kresse, G., Vocado, L., Dobson, D., Alfe, D., Gillan, M. J. & Price, G. D. 1998 The viscosity of liquid iron at the physical conditions of the Earth's core. *Nature* **392**, 805–807.

- Fearn, D. R. 1998 Hydromagnetic flow in planetary cores. *Rep. Prog. Phys.* **61**, 175–235.
- Glatzmaier, G. A. & Roberts, P. H. 1995 A three-dimensional convective dynamo solution with rotating and finitely conducting inner core and mantle. *Phys. Earth Planet. Interiors* **91**, 63–75.
- Glatzmaier, G. A. & Roberts, P. H. 1997 Simulating the geodynamo. *Contemp. Phys.* **38**, 269–288.
- Glatzmaier, G. A., Coe, R. S., Hongre, L. & Roberts, P. H. 1999 The role of the Earth's mantle in controlling the frequency of geomagnetic reversals. *Nature* **401**, 885–890.
- Gubbins, D. & Bloxham, J. 1987 Morphology of the geomagnetic field and implications for the geodynamo. *Nature* **325**, 509–511.
- Hollerbach, R. 1996 On the theory of the geodynamo. *Phys. Earth Planet. Interiors* **98**, 163–185.
- Hollerbach, R. 2000 A spectral solution of the magnetoconvection equations in spherical geometry. *Int. J. Numer. Meth. Fluids*. (In the press.)
- Hollerbach, R. & Jones, C. A. 1993 Influence of the Earth's inner core on geomagnetic fluctuations and reversals. *Nature* **365**, 541–543.
- Jones, C. A., Longbottom, A. W. & Hollerbach, R. 1995 A self-consistent convection driven geodynamo model using a mean field approximation. *Phys. Earth Planet. Interiors* **92**, 119–141.
- Jones, C. A., Soward, A. M. & Mussa, A. I. 2000 The onset of thermal convection in a rapidly rotating sphere. *J. Fluid. Mech.* **405**, 157–159.
- Kageyama, A. & Sato, T. 1997a Generation mechanism of a dipole field by a magnetohydrodynamical dynamo. *Phys. Rev. E* **55**, 4617–4626.
- Kageyama, A. & Sato, T. 1997b Dipole field generation by an MHD dynamo. *Plasma Phys. Control. Fusion* **39**, 83–91.
- Kageyama, A. & Sato, T. 1997c Velocity and magnetic field structures in a magnetohydrodynamic dynamo. *Phys. Plasmas* **4**, 1569–1575.
- Katayama, J. S., Matsushima, M. & Honkura, Y. 1999 Some characteristics of magnetic field behavior in a model of MHD dynamo thermally driven in a rotating spherical shell. *Phys. Earth Planet. Interiors* **111**, 141–159.
- Kitauchi, H. & Kida, S. 1998 Intensification of magnetic field by concentrate-and-stretch of magnetic flux lines. *Phys. Fluids* **10**, 457–468.
- Kida, S. & Kitauchi, H. 1998a Thermally driven MHD dynamo in a rotating spherical shell. *Prog. Theor. Phys. Suppl.* **130**, 121–136.
- Kida, S. & Kitauchi, H. 1998b Chaotic reversals of dipole moment of thermally driven magnetic field in a rotating spherical shell. *J. Phys. Soc. Jap.* **67**, 2950–2951.
- Kuang, W. & Bloxham, J. 1997 An Earth-like numerical dynamo model. *Nature* **389**, 371–374.
- Kuang, W. & Bloxham, J. 1999 Numerical modelling of magnetohydrodynamic convection in a rapidly rotating spherical shell. I. weak and strong field dynamo action. *J. Comp. Phys* **153**, 51–81.
- Lesur, V. & Gubbins, D. 1999 Evaluation of fast spherical transforms for geophysical applications. *Geophys. J. Int.* **139**, 547–555.
- Longbottom, A. W., Jones, C. A. & Hollerbach, R. 1995 Linear magnetoconvection in a rotating spherical shell, incorporating a finitely conducting inner core. *Geophys. Astrophys. Fluid Dynam.* **80**, 205–227.
- Malkus, W. V. R. & Proctor, M. R. E. 1975 The macrodynamics of  $\alpha$ -effect dynamos in rotating fluids. *J. Fluid Mech.* **67**, 417–444.
- Morrison, G. & Fearn, D. R. 2000 The influence of Rayleigh number, azimuthal wave-number and inner core radius on 2.5D hydromagnetic dynamos. *Phys. Earth Planet. Interiors.* **117**, 237–258.
- Olson, P. & Glatzmaier, G. A. 1995 Magnetoconvection and thermal coupling of the Earth's core and mantle. *Phil. Trans. R. Soc. Lond. A* **354**, 1413–1424.

- Olson, P., Christensen, U. & Glatzmaier, G. A. 1999 Numerical modeling of the geodynamo: mechanisms of field generation and equilibration. *J. Geophys. Res.* **104**, 10383–10404.
- Roberts, P. H. 1994 Fundamentals of dynamo theory. *Lectures on solar and planetary dynamos* (ed. M. R. E. Proctor & A. D. Gilbert), pp. 1–58. Cambridge University Press.
- Roberts, P. H. & Gubbins, D. 1987 Origin of the main field. Kinematics. *Geomagnetism* (ed. J. A. Jacobs), vol. 2, pp. 185–249. Academic.
- Roberts, P. H. & Soward, A. M. 1992 Dynamo theory. *A. Rev. Fluid Mech.* **24**, 459–512.
- Sakuraba, A. & Kono, M. 1999 Effect of the inner core on the numerical solution of the magnetohydrodynamic dynamo. *Phys. Earth Planet. Interiors* **111**, 105–121.
- Sarson, G. R. & Jones, C. A. 1999 A convection driven geodynamo reversal model. *Phys. Earth Planet. Interiors* **111**, 3–20.
- Sarson, G. R., Jones, C. A. & Longbottom, A. W. 1997a The influence of boundary region heterogeneities on the geodynamo. *Phys. Earth Planet. Interiors* **101**, 13–32.
- Sarson, G. R., Jones, C. A., Zhang, K. & Schubert, G. 1997b Magnetoconvection dynamos and the magnetic fields of Io and Ganymede. *Science* **276**, 1106–1108.
- Sarson, G. R., Jones, C. A. & Longbottom, A. W. 1998 Convection driven geodynamo models of varying Ekman number. *Geophys. Astrophys. Fluid Dynam.* **88**, 225–259.
- Schubert, G., Zhang, K., Kivelson, M. G. & Anderson, J. D. 1996 The magnetic field and internal structure of Ganymede. *Nature* **384**, 544–545.
- Stevenson, D. J. 1979 Turbulent thermal convection in the presence of rotation and a magnetic field: a heuristic theory. *Geophys. Astrophys. Fluid Dynam.* **12**, 139–169.
- Taylor, J. B. 1963 The magneto-hydrodynamics of a rotating fluid and the earth's dynamo problem. *Proc. R. Soc. Lond. A* **274**, 274–283.
- Tilgner, A. 1997 A kinematic dynamo with a small scale velocity field. *Phys. Lett. A* **226**, 75–79.
- Walker, M. R., Barenghi, C. F. & Jones, C. A. 1998 A note on dynamo action at asymptotically small Ekman number. *Geophys. Astrophys. Fluid Dynam.* **88**, 261–275.
- Zhang, K. 1991 Convection in a rapidly rotating spherical shell at infinite Prandtl number: steadily drifting rolls. *Phys. Earth Planet. Interiors* **68**, 156–169.
- Zhang, K. & Busse, F. H. 1989 Convection driven magnetohydrodynamic dynamos in rotating spherical shells. *Geophys. Astrophys. Fluid Dynam.* **49**, 97–116.
- Zhang, K. & Gubbins, D. 1993 Convection in a rotating spherical fluid shell with an inhomogeneous temperature boundary condition at infinite Prandtl number. *J. Fluid Mech.* **250**, 209–232.
- Zhang, K. & Gubbins, D. 2000 Is the dynamo intrinsically unstable? *Geophys. J. Int.* (In the press.)
- Zhang, K. & Jones, C. A. 1997 The effect of hyperviscosity on geodynamo models. *Geophys. Res. Lett.* **24**, 2869–2872.